J Solid State Electrochem (2009) 13:245–261
DOI 10.1007/s10008-008-0554-y

ORIGINAL PAPER

Self-organization in nonlinear dynamical systems and its relation to the materials science

Marek Orlik

Received: 13 December 2007 / Accepted: 18 March 2008 / Published online: 25 April 2008

Abstract This review paper presents briefly the main concepts of nonlinear dynamics and their exemplary manifestations in selected systems, including those important from the point of view of materials science. It is an extended version of the conference presentation. The conditions of instabilities leading to spontaneous formation of dissipative structures are given. Principles of nonlinear dynamics are illustrated with several examples from the homogeneous and heterogeneous and physical and chemical systems: pattern formation in the convective motion of fluids subject to various kinds of driving forces, periodic precipitation phenomena, oscillations, and pattern formation in the Belousov–Zhabotinski (BZ) reaction and the catalytic oxidation of thiocyanate ions with hydrogen peroxide, as well as bistability and tristability in the electrochemical reduction of azide complexes of nickel (II). The application of nonlinear dynamics in materials science is first exemplified by its role in polymerization reactions. Such processes can either exhibit internal couplings leading to oscillations or can be coupled with the chemical oscillatory process through, e.g., the covalent bonding of its catalyst to the polymer network. Other selected examples of the application of nonlinear dynamics in materials science, referring to electrochemical processes, were briefly reviewed. Nonlinear dynamics appears to be useful for designing new materials, including those at the nanoscale.

M. Orlik (✉)
Faculty of Chemistry, University of Warsaw,
ul. Pasteura 1,
02-093 Warsaw, Poland
e-mail: morlik@chem.uw.edu.pl

Keywords Nonlinear dynamics · Dissipative structures · Self-organization · Oscillations · Multistability · Materials science · Polymer chemistry · Electrochemical micromachining · Nanostructures

Introduction

This concise lecture is basically addressed to the audience that is not familiar with nonlinear dynamics but is interested in the application of its concepts in materials science. Therefore, the presentation begins from a quite simple, even traditional introduction into the basic concepts of nonlinear dynamics. It is then followed by typical examples of nonlinear behavior in chemical and electrochemical systems. Finally, selected examples of manifestation of nonlinear dynamics in the processes related to the materials sciences: polymer chemistry and electrochemical preparations of nanomaterials, are collected. This review does not pretend to be an exhaustive source of information on this intensively developing discipline but should anyway introduce the audience into the applications of nonlinear dynamics in the preparation of chemical materials of desired properties and encourage to further searches and studies.

The subject and basic concepts of nonlinear dynamics

Many physical, chemical, biological, and even social processes exhibit nonlinear dynamic characteristics, in the sense of the dependence between the magnitude of the driving forces and the intensity of the resulting flows. Of course, there are many processes that within a certain range of driving forces can be considered *practically*

linear, as, e.g., the Fick's law of diffusion. If this is the case, significant simplification of theoretical considerations is possible, and mathematical (differential) equations underlying such linearized behavior in many cases can be solved analytically. The nonlinear problems, however, due to the lack of mathematical tools were for a long time neglected or insistently linearized. Only the progress in numerical computing techniques, which occurred in recent decades, as well as the invention of advanced experimental techniques, caused substantial development in the studies of nonlinear phenomena.

What are the consequences of nonlinearity in the systems' dynamics? If certain additional conditions, which will be listed below, are met, the behavior of the dynamical system can undergo spontaneous *self-organization*, and, as a result of which (after Prigogine), the *dissipative structures* are formed. The second law of thermodynamics describes these phenomena in the following way: the decrease in the system's entropy due to the structure formation has to be overcome by the entropy produced by the parallel irreversible (dissipative) process.

There are different kinds of dissipative structures. First, if the entire system's state starts to oscillate uniformly, such a dynamic behavior is a manifestation of the *temporal* (i.e., developing as a function of time) *dissipative structure*. These oscillatory changes of state can be either periodic or aperiodic; in the latter case, they can represent a particularly interesting phenomenon of the deterministic chaos, i.e., apparently completely disordered oscillations, but with the hidden and very complex order. Second, if the state of the system changes (in an oscillatory manner) as a function of not only time but also of the spatial coordinates, the traveling fronts, "chemical waves," or—more generally—the *spatiotemporal patterns* are formed. Third, if the development of the structure stops and in this way the stationary pattern emerges (although dissipative processes are constantly running), the spatial dissipative pattern appears in the system. One of the most important (and now intensively studied) types of such structures are the *Turing patterns*, which appear as a result of specific coupling between the kinetics of chemical reactions and the diffusion transport of reagents. For the literature on theory and experimental characteristics of the chemical oscillatory processes, the reader is advised to consult, e.g., [1–4].

Another typical nonlinear phenomenon, frequently very closely related to the oscillations, is *multistability*, which means that for the same range of control parameters (as, e.g., the flow rate through the tank reactors or the voltage applied between the electrodes), it is possible to place the system in one of multiple stable steady states. Which of the possible steady states is attained in a given experiment depends on the "history" of the system, i.e., whether the control parameter was increasing or decreasing to the same final value. This, in turn, means that multistability manifests itself experimentally as the hysteresis in the system's behavior upon cyclic changes of the control parameter. Obviously, such situation cannot occur in equilibrium, which state is unambiguously defined. The simplest case of multistability, bistability, observed in quite numerous nonlinear systems, means the coexistence of only two stable steady states (see Fig. 1).

All such transitions between the "trivial" steady state and spontaneous formation of dissipative structures are associated with the respective *bifurcations*. This essentially mathematical term, related to the characters of the solutions of differential equations, means in its simplest, intuitive sense—the qualitative change of the solutions of such equations that occurs upon variation of the equation parameters. For example, the transition between the trivial monostable and the bistable (multistable) behavior is associated with the so-called saddle-node bifurcations. The name of this bifurcation comes from the types of the phase trajectories that appear in the phase space of the dynamical system, upon the parameters' change. As a result of a single saddle-node bifurcation, the pair of steady states in the phase space is born, one that is stable and with trajectories leading to it having a shape suggesting the name of a node and the other steady state that is unstable, with phase trajectories around it forming a shape reminding one of a saddle. The oscillatory behavior may arise as a result of various bifurcations. Of particular importance is the frequently occurring Hopf bifurcation, associated with the loss of stability of the single steady state (fixed point in mathematical terms) and the appearance of the cyclic phase trajectory (limit cycle) around it. Of course, cyclic trajectories in the phase space correspond to the oscillatory behavior.

The stable and unstable regimes of dynamical behavior, in terms of their representation in the phase space, are also called the attractors and the repellors, respectively. The

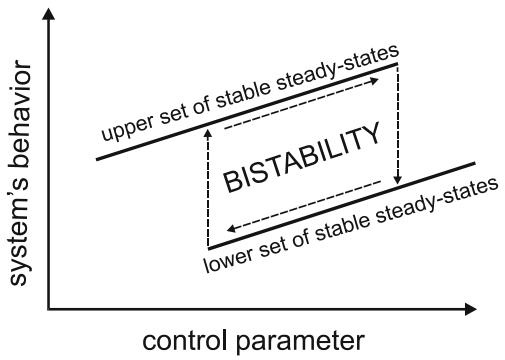

Fig. 1 Schematic manifestation of bistability as the hysteresis of the system's behavior upon cyclic changes of the control parameter

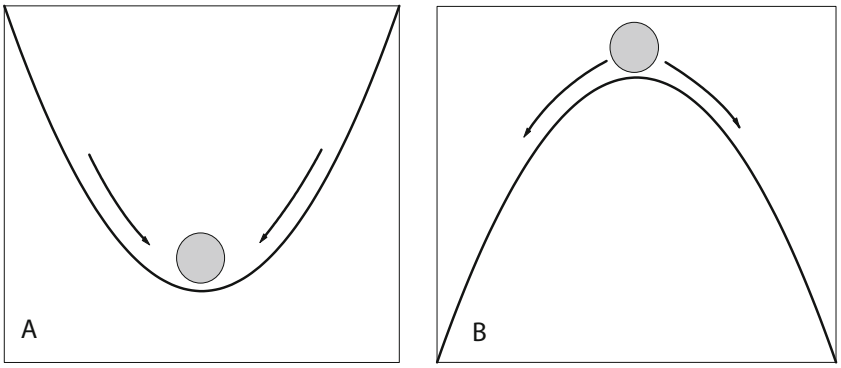

Fig. 2 Schematic representation of **a** the stable steady state (an attractor) and **b** the unstable steady state (a repellor). For the attractor, the perturbations of the steady state are asymptotically damped, whereas for the repellor, they are amplified, and the system switches to another state (not explicitly defined in the figure)

point attractor in a phase space corresponds to a single steady state, and the simplest cyclic attractor corresponds to periodic stable oscillations. More complicated shapes correspond to appropriately more complex oscillations, including eventually chaotic phase portraits that, if they correspond to the abovementioned deterministic chaos, are called the *strange attractors*. The repellor is just the reverse concept—all the trajectories drive the system away from this state, which in this way has a "repulsive" nature. For the simple illustration of the idea of the attractor and the repellor, see Fig. 2.

It is noteworthy that the analysis of various dynamical systems, very different in their physical or chemical (or any other) characteristics, shows that their dynamical behaviors exhibit similarities in terms of the bifurcation schemes. These universalities are one of the most important and fascinating features of the dynamical systems, which also are one of the manifestations of the unity of nature.

As stated above, nonlinear dynamics is observed in many systems of very different kinds, including living organisms that can be considered the most complicated dissipative structures. One of relatively new applications of nonlinear dynamics is its increasing role in materials science, where it serves both as a tool for understanding the course of chemical syntheses in various types of reactors and for designing new materials of special properties.

This presentation is further devoted to the short description of selected chemical dynamical systems, including the results of our own research in this area. These considerations will be further followed by the outline description of the role of nonlinear dynamics in materials science.

Conditions of oscillations and pattern formation in chemical systems

The analysis of known systems exhibiting various kinds of dynamic instabilities leads to the conclusion that the formation of dissipative structures requires meeting of the following conditions:

1. The main process has to be irreversible and thus characterized with large negative ΔG, which condition, according to basic thermodynamics, is equivalent to the increase in entropy of both the system and its surroundings; as stated above, the entropy-producing dissipative reaction allows the structure formation to manifest itself, as long as this dissipation occurs.
2. The kinetic characteristics of the system dynamics should be nonlinear (i.e., the reaction rate should be, e.g., a quadratic function of reagents' concentrations).[1]
3. The steps of the kinetic reaction mechanism should include positive (autocatalysis) and/or negative (autoinhibition) feedback loops.

As a particularly simple model reaction scheme, which meets all the above conditions and generates sustained oscillations, one can invoke the classical Lotka–Volterra (L-V) mechanism, which was originally proposed for the description of the "predator–victim" processes in nature.

The L-V model consists of the two autocatalytic steps, representing the reproduction of the intermediates X and Y, respectively, and the third step involving the irreversible decay of Y to the final product B.

$$\mathrm{A} + \mathrm{X} \xrightarrow{k_1} 2\mathrm{X} \quad \text{(autocatalytic production of X)} \tag{1}$$

$$\mathrm{X} + \mathrm{Y} \xrightarrow{k_2} 2\mathrm{Y} \quad \text{(autocatalytic production of Y)} \tag{2}$$

$$\mathrm{Y} \xrightarrow{k_3} \mathrm{B} \quad \text{(irreversible decay of Y)} \tag{3}$$

The sum of all the three elementary steps yields the overall, stoichiometrically simple equation of the irrevers-

[1] An exception from this condition is thermal diffusion, which characteristics are practically linear under a typical condition, although it can cause dissipative separation of a mixture of gases of different molecular masses, in the temperature field.

ible transformation: A→B. We further assume that reactant A is constantly supplied to the reactor, so its concentration remains unchanged during the reaction course: [A]=const. However, the concentrations of X and Y can oscillate as a function of time.

If the differential kinetic equations for the d[X]/dt and d[Y]/dt do not include the terms corresponding to the spatial distribution (and thus diffusion) of those species, the whole problem is simplified to the ordinary differential equations, describing the isotropic dynamics of the entire system's state. Typical oscillatory solutions for [X] and [Y] species, exhibiting the phase shift, are shown in Fig. 3. One can understand these oscillations as an interplay of the alternating dominance of the positive and the negative feedback loops in the reaction mechanism. According to Eq. 1, the production of X from A is autocatalytically accelerated. When the concentration of X attains a sufficiently high value, the autocatalytic production of Y (according to Eq. 2) starts abruptly, but this means also that the X species is quickly consumed. This, in turn, slows down the autocatalytic production of Y, which then only irreversibly decays (cf. Eq. 3), until reaction 1 again supplies the next portions of X and the whole cycle repeats. In spite of remarkable didactic features, the weakness of this model is that the oscillations are not asymptotically stable; that is, the perturbations are not damped as a function of time (cf. Fig. 2a). Since they do not either exponentially diverge, the system is classified as stable in the Lapunov sense. It may be also called the conservative but not the dissipative system. However, subtle extensions of this mechanism can make it a dissipative one.

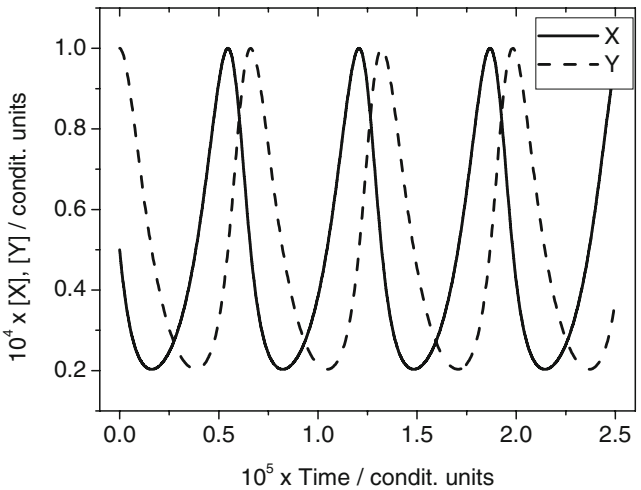

Fig. 3 Sustained oscillatory changes of the concentrations of the X and Y intermediates for the L-V mechanism (*1–3*), with the following model parameters: $k_1 = k_3 = 1 \times 10^{-4}$; $k_2 = 2 \times 10^{-8}$, [A]=1, $[X]_0$=5,000, $[Y]_0$=10,000. The fourth-order Runge–Kutta method was used for the numerical integration of kinetic equations

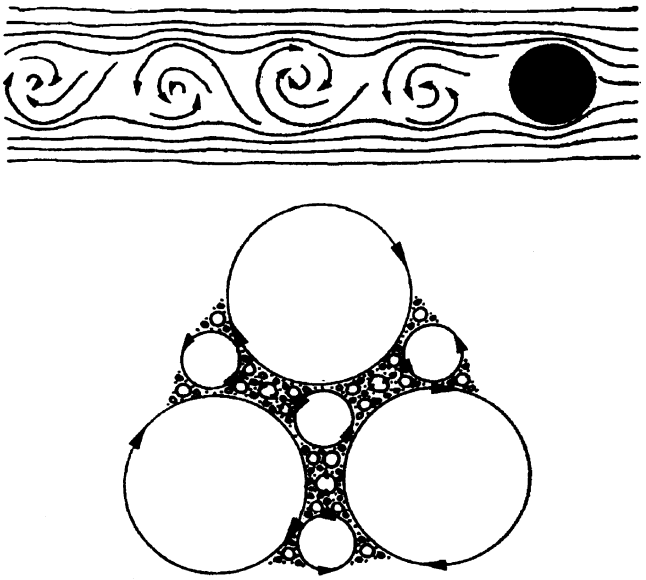

Fig. 4 The scheme of formation of the Bénard–von Karman trails in the stream of fluid meeting an obstacle and the fractal population of vortices observed for the conditions of the turbulent flow [3]

Examples of dissipative structures in selected chemical systems

Following the abovementioned model of the oscillatory system, the selected examples of the real dissipative structures will be now briefly reviewed.

Self-organization in the convective motion of fluid

Bénard–von Karman trails

The apparently trivial flow of water in the stream coming across an obstacle (like a vertically put rod) exhibits self-organization of vortices, which form the so-called Bénard–von Karman trails (see Fig. 4). If the flow becomes intensive enough, the population of vortices becomes so complicated that it looks apparently completely chaotic, although in fact it is an example of the deterministic chaos. The population of vortices reveals then the *fractal*, i.e., *self-similar* nature. The fractals, which term was introduced by B. Mandelbrot, can be considered the geometric picture of deterministic chaos. Many fractals are surprisingly beautiful.

Convective cells in the density-driven convection

Remarkable self-organization of convection is observed in the thin layer of the fluids. The driving force for this kind of convection can have different origins. One of them is the density gradient that can be, in turn, caused by either the temperature gradient (even for pure fluids) or by the concentration gradient (for the solutions, when the system

can be isothermal). If the density of the upper zone of the fluid is greater than that of its lower zone, in the gravitational field, the nonequilibrium situation develops, the internal pressure appears, and there is a natural tendency for the fluid zones to exchange their places. In the simplest case, this exchange takes a form of cooperating convective rolls (Fig. 5). Typically, the diameter of the cross-section of every roll is close to the distance between the plates, so the characteristic size of the convective patterns of that type is largely determined by this distance.

Under specific conditions, particularly if the upper surface of the fluid is free (i.e., not covered), such a convective motion may take a form of hexagonal cells, reported for the first time in 1900 by Henri Bénard. The spatial distribution of the convective cells resembles then the structure of a honeycomb.

Self-organization in the electrohydrodynamic convection

Another type of the driving force for the convective phenomena comes from the little violation of the electroneutrality condition during the thin-layer electrolysis of the solutions of a low concentration of ions (i.e., of high ohmic solution resistance). The product of the spatial charge density and the local electric field creates the volume electric force in the fluid, which is a cause for the electrohydrodynamic (EHD) convection. This phenomenon occurs, e.g., in the thin layer of the liquid crystals placed in the electric field, and the resulting spatial (dissipative) patterns are called the Williams domains [5]. Another example of the EHD convection was discovered by Schaper et al. from the Philips Laboratory in Aachen, who performed the thin-layer (d=100–200 μm) electrolysis of the solution of rubrene in 1,2-dimethoxyethane, with a very small amount of ionic salt [6]. The principle of this

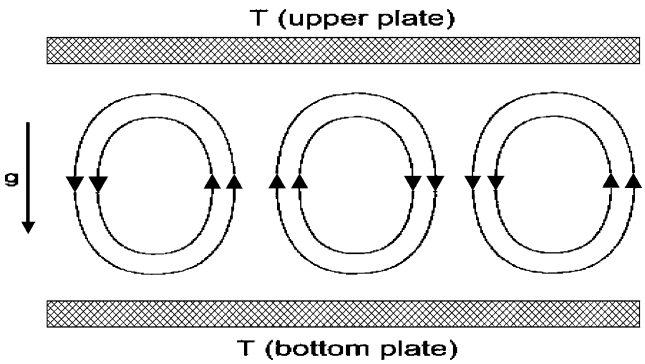

Fig. 5 The schematic geometry of the cooperating convective rolls, developing in the thin layer of the fluid, heated from below (temperature gradient $\Delta T = T$(bottom plate)$-T$(upper plate)>0), so the density of the upper zone is greater than that of the lower zone. Quasi-circular cross-section of every roll is largely determined by the distance between the plates (adapted from [3])

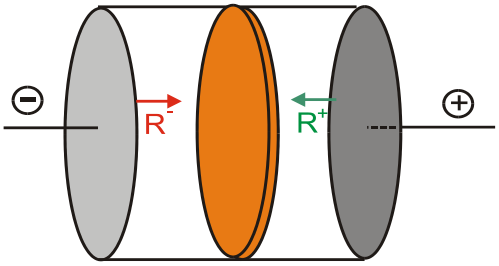

Fig. 6 Schematic picture of the electrolysis of rubrene (R) between the two parallel electrodes at which the radical anions (R^-) and radical cations (R^+) appear. The diffusion and migration of both ions toward each other causes their recombination in the solution bulk with the evolution of orange light

experiment is sketched in Fig. 6. Rubrene cations and anions, formed at the respective electrodes, diffuse and migrate toward each other, and when they meet, they recombine with the evolution of orange light (this is one of the handbook examples of electrochemiluminescence).

It is surprising to note that instead of a middle homogeneous layer of luminescence, as suggested by the simplified Fig. 6, Schaper et al. observed a quasi-hexagonal pattern of orange light, associated with the visible motion of the fluid. The similarity of the morphology of these newly discovered patterns to the classical Bénard phenomenon was striking, but the driving force had to be assumed differently—as the EHD one. Later, we undertook further studies of this subject, to find possible types of the convective structures in this system and to elaborate the qualitative and quantitative mechanisms of these phenom-

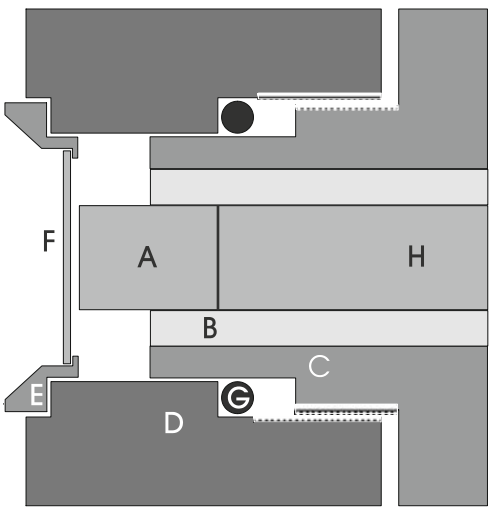

Fig. 7 Schematic cross-section of the thin-layer electrolytic cell. Symbols: *A*—copper electrode, *B*—KEL-F insulating layer, *C*—metallic (bronze and steel) movable block, *D*—metallic (bronze) fixed block connected with part C by the thread, *E*—steel ring for fixing the glass electrode, *F*—transparent electrode (glass plate coated from inside with the transparent semiconducting ITO layer), *G*—sealing O-ring, *H*—copper rod (reprinted with permission from [7], Copyright 1998 American Chemical Society)

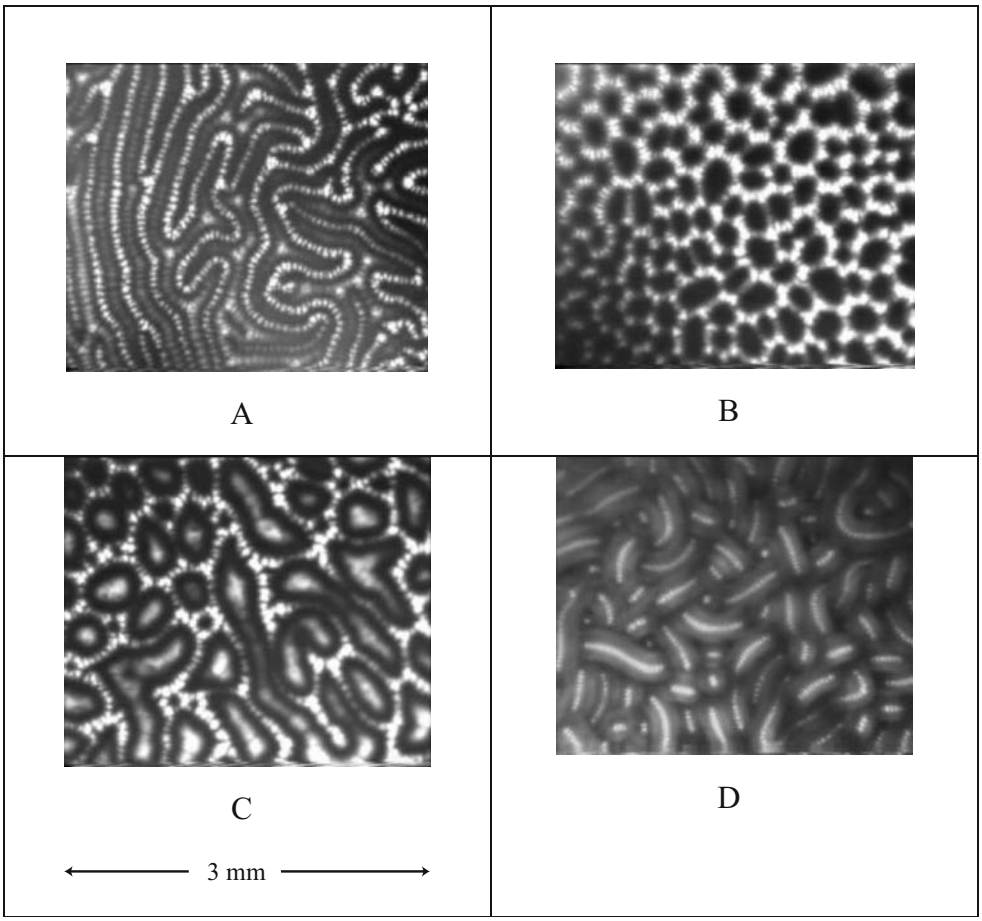

Fig. 8 Exemplary convective patterns observed (through the transparent electrode) during the electrolysis of rubrene ($c_R = 4 \times 10^{-3}$ M) dissolved in 1,2-dimethoxyethane, in the thin-layer cell from Fig. 7, for various voltages U=4.0–4.5 V between the electrodes, interelectrode distances d=80–120 μm, and concentrations of tetrabutylammonium hexafluorophosphate as a supporting electrolyte $c_{se} = 6.0 \times 10^{-6} - 2 \times 10^{-5}$ M. *Bright zones* correspond to orange light of rubrene electrochemiluminescence; **a** "fingerprints," **b** hexagonal patterns (reprinted in part with permission from [7], Copyright 1998 American Chemical Society), **c** spatial chaos in cellular convection [10] (reproduced by permission of the PCCP Owner Societies), **d** worm-like patterns

ena in terms of the appropriate numerical models [7–11]. Our thin-layer electrochemical cell is schematically shown in Fig. 7. Typical luminescent electroconvective structures, reported in our experiments, are collected in Fig. 8.

To confirm the mechanism of the formation of these luminescent patterns, we performed the possibly realistic numerical calculation of the driving force [8], followed by modeling of the fluid motion in the two-dimensional space, in terms of the Navier–Stokes equation [9]. Figure 9 schematically explains how the formation of convective rolls can be extended for the creation of zones of luminescence (indicated by asterisks), where the local

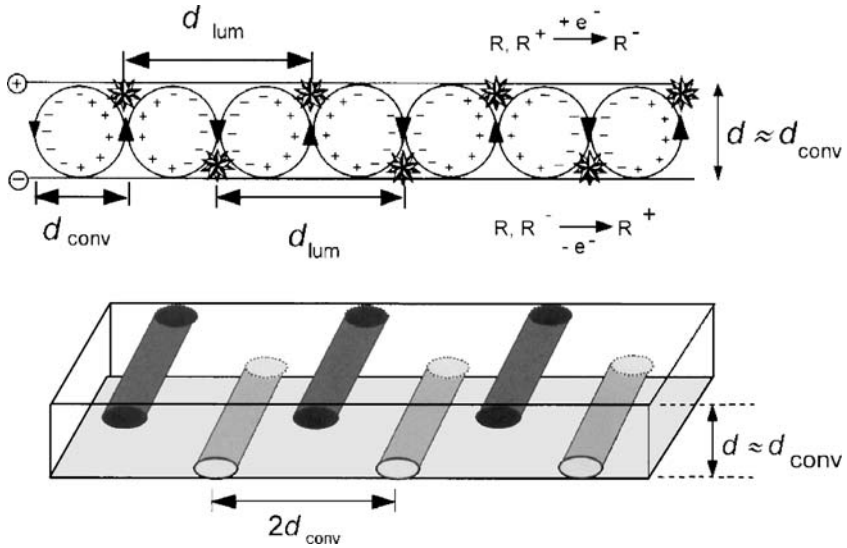

Fig. 9 Mechanism of generation of linear patterns of luminescence exhibiting the spatial period (d_{lum}) doubling the interelectrode distance (d): *Top part*, visible luminescence (*asterisks*) occurs where the convective streams carrying rubrene ions formed at one electrode approach the other electrode; *bottom part*, three-dimensional distribution of cathodic-anodic luminescence; the traces in the cathodic and anodic layers are mutually shifted for the value comparable with the interelectrode distance d in the plane parallel to the electrodes (reprinted with permission from [7], Copyright 1998 American Chemical Society)

product of R^+ and R^- concentrations is expected to be the highest. In turn, Fig. 10 explains the shape of the luminescent hexagonal patterns, indicating in particular that the hexagonal shape is formed at one electrode, while, at the opposite electrode, only the centrally positioned spot should be visible. One should emphasize that this imagination was confirmed by our experimental results in which the conditions allowed us to record the hexagonal patterns associated with the luminescence occurring simultaneously at both electrodes (cf. upper left corner of the Fig. 8c).

In turn, Fig. 11 shows the course of the numerical modeling of the self-organized convection in the two-dimensional thin-layer system, which is initially homogeneous. The centrally imposed fluctuation of the solution resistance soon initiates the first pair of the counter-rotating convective rolls, which, as a function of time, agitate further portions of the solution. Eventually, practically the entire interelectrode space becomes engaged in the set of cooperating convective rolls.

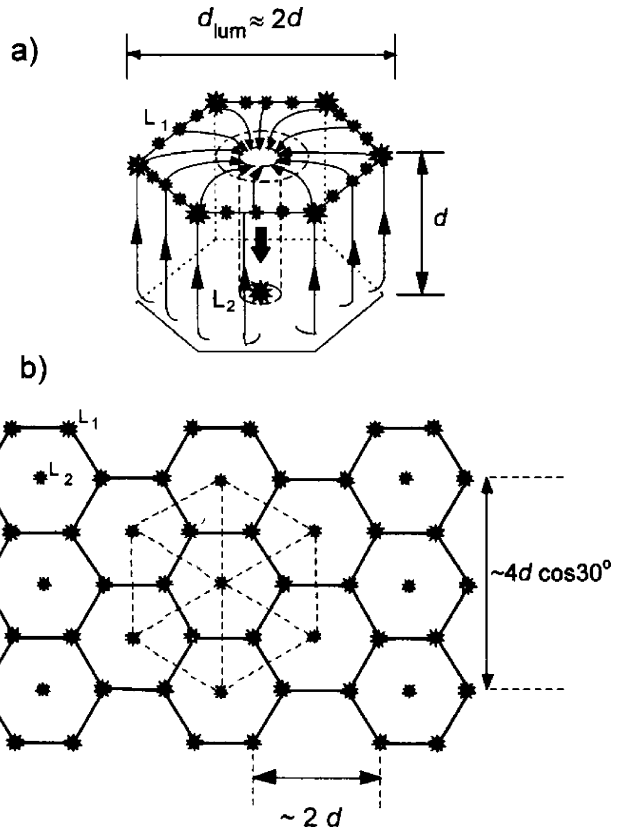

Fig. 10 **a** Schematic shapes of convective flows, forming a single convective cell, manifesting itself as an hexagonal arrangement of luminescence at one electrode, with a predicted central spot at the opposite electrode; **b** corresponding expected schematic view of the luminescent solution, observed through the transparent electrode [10] (reproduced by permission of the PCCP Owner Societies)

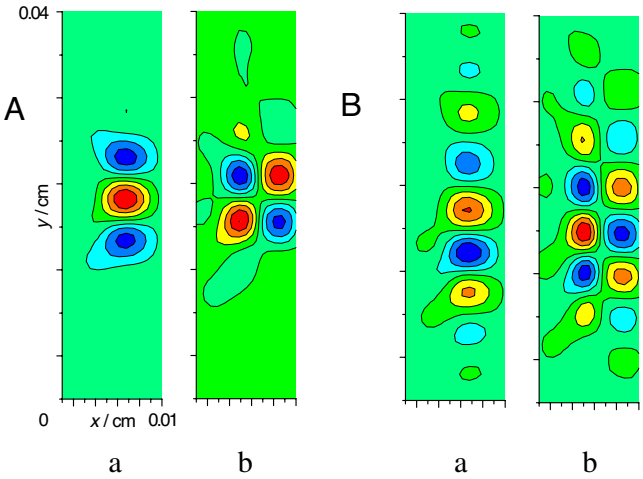

Fig. 11 Numerical modeling of the progress of self-organization in the evolution of EHD convection as a function of time, shown in terms of the *x*-component (*a*) and the *y*-component (*b*) of a fluid velocity. The local fluctuation introduced in the middle of the model system (**a**) gives rise to the first pair of the cooperating, counter-rotating rolls. **b** As a function of time, the entire solution becomes engaged in convective motion in the form of the cooperating rolls. Reprinted from [11], Copyright 2000, with permission from Elsevier

Oscillations and pattern formation in chemical reactions

The periodic precipitation in gel media (the Liesegang phenomena)

A typical laboratory example is the formation of circular patterns of the Ag_2CrO_4 precipitate formed in the K_2CrO_4-containing gelatin layer around the drop of aqueous solution of $AgNO_3$, put on it. In nature, one can easily find this kind of spatial dissipative structures in the cross-section of such minerals like ribbon agate (see Fig. 12) or

Fig. 12 The Liesegang bands in the ribbon agates (photo made by the author)

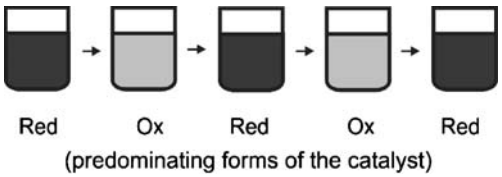

Fig. 13 Schematic representation of the periodic variations of the color of the solution in which the BZ reaction proceeds, catalyzed either by the Ce(III)/Ce(IV) couple (solution turns from colorless into yellow) or by the ferroin/ferriin couple (solution color oscillates between the dark red and blue)

malachite. These patterns developed when the minerals were still in the state of magma.

Temporal and spatiotemporal dissipative structures in the oscillatory Belousov–Zhabotinski reaction

The Belousov–Zhabotinski (BZ) process, discovered in 1958 by B. P. Belousov, is by no means the most famous oscillatory process that occurs during the oxidation of various organic compounds by bromate(V) ions in acidic media, provided that the appropriate catalyst is present in the solution. Typical composition, recommended, e.g., for the lecture demonstrations, involves potassium bromate(V), malonic acid, sulfuric acid (ensuring the acidic medium), and the Fe(III)/Fe(II) (as ferroin/ferriin) or Ce(IV)/Ce(III) catalytic redox couple. If the solution is efficiently stirred, its color changes periodically as a function of time, as Fig. 13 schematically shows. The period of these oscillations is usually of the order of approximately tenths of seconds to a few minutes, in dependence of the reagent concentrations and the catalyst used.

If the same process is performed in the thin layer (d=1–2 mm) of the solution placed in the typical Petri dish (with the upper surface free), the particularly fascinating population of spatiotemporal patterns (traveling concentration waves) develops. If ferroin is used as a catalyst, in the initially uniformly red solution, the blue points (indicating the local enhancement of the Fe(III) complex) appear in random places, and they soon develop into the sets of the concentric circular waves (Fig. 14). These phenomena are considered a simple chemical model of morphogenesis when initially identical cells acquire chemical information, differentiate, and build up specialized tissues.

The BZ process has been the most intensively studied oscillatory reaction for almost 50 years, under various conditions, in different reactors (batch, flow, coupled) and gels replacing water as the reaction medium. In the flow reactors, one can observe not only oscillations but also bistability.

Another important class of homogeneous oscillators involves hydrogen peroxide as the oxidant for, among others, thiocyanates, thiosulfates, or sulfides. In this review, we refer to the first of these systems, discovered in 1986 by Orbán [12], as the rare example of the oscillatory process, occurring both under batch and flow conditions. Very recently, we found that this process can be also a source of spatiotemporal patterns, visualized by blue luminescence emitted upon the addition of luminol to a thin layer of the solution placed between the two glass plates [13]. Figure 15 shows the series of photographs of this phenomenon, indicating its striking periodicity. The time of evolution of pictures composing Fig. 15 is equal to approximately 25 min. The role of various factors in the formation of these chemical waves, including convection, will be a subject of our further studies.

At the end of this chapter, one should note that the mentioned earlier Turing patterns are recently more and more intensively studied, both in homogeneous and heterogeneous (e.g., electrochemical) systems. According to the Turing definition, they are a result of a specific coupling of the kinetics of chemical reaction and diffusion transport that occurs (it is one of the conditions) if the diffusion coefficients of the reacting species are different. If the transport other than diffusion (e.g., migration) is involved in the formation of such stationary dissipative structures, they should be called the *Turing-like patterns*, as

Fig. 14 The onset and the development of spatiotemporal dissipative patterns (chemical waves) in the ferroin-catalyzed BZ process, performed in the thin layer of the solution, placed in the Petri dish (experiments performed and pictures taken by © Dr. T. Pluciński, University of Gdańsk, Poland, reproduced with kind permission of the author)

the original Turing definition refers to diffusion only. So far, Turing patterns were found both in model calculations and experimental systems, offering frequently visually nice pictures.

Oscillations and multistability in electrochemical systems

There are numerous examples of oscillations and bistability in various electrode processes, including deposition of solid materials on the surfaces or dissolution of electrode materials. In fact, electrochemical oscillations were probably the first such instabilities, observed experimentally, as the reports on such phenomena were published already in the nineteenth century. The famous example was the oscillatory dissolution of iron electrodes in acidic media, the simplified mechanism of which was in these early works attributed to the cyclic variations of the corrosion (Flade) potential, caused by periodic variation of the solution pH at the electrode.

In this chapter, we shall further refer to our recent works with the electroreduction of the azide complexes of nickel (II) at the *streaming mercury electrode* [14]. Such an electrode [15] ensured both the constant inflow of the reactants and constant removal of the reaction products, so the system could attain a true steady state before the onset of instability, leading to multistability or oscillations. The solution containing azide complexes of Ni(II), which is a mixture of $Ni(ClO_4)_2$ and excess amount of NaN_3, must be also slightly acidified (with $HClO_4$), since otherwise it remains turbid due to hydroxo-forms of nickel(II). It appears that such a composition of the sample causes its quite unique current–potential (*I–E*) characteristics, exhibiting two regions of the *N*-shaped negative differential resistance (NDR), as Fig. 16 shows. The NDR $= dE/dI < 0$ means that in a certain potential range, in spite of its increasing negative value (i.e., increasing driving force for the reduction process), the reduction current becomes less negative; that is, the rate of the process decreases. In our work [16], we were able to explain the shape of this characteristics as coming from the parallel reduction of the central Ni(II) ion and partial reduction of the azide ligand, the latter one occurring at more negative potentials. The main process, Ni(II) reduction, forms the *I–E* response with the single NDR region, which is deformed by the small postwave of azide reduction in such a way that two NDR regions eventually develop.

The existence of two NDR regions immediately suggests the possibility of not only bistability (for which a single NDR region is sufficient) but also *tristability*, i.e., the coexistence of the three stable steady states for the same set

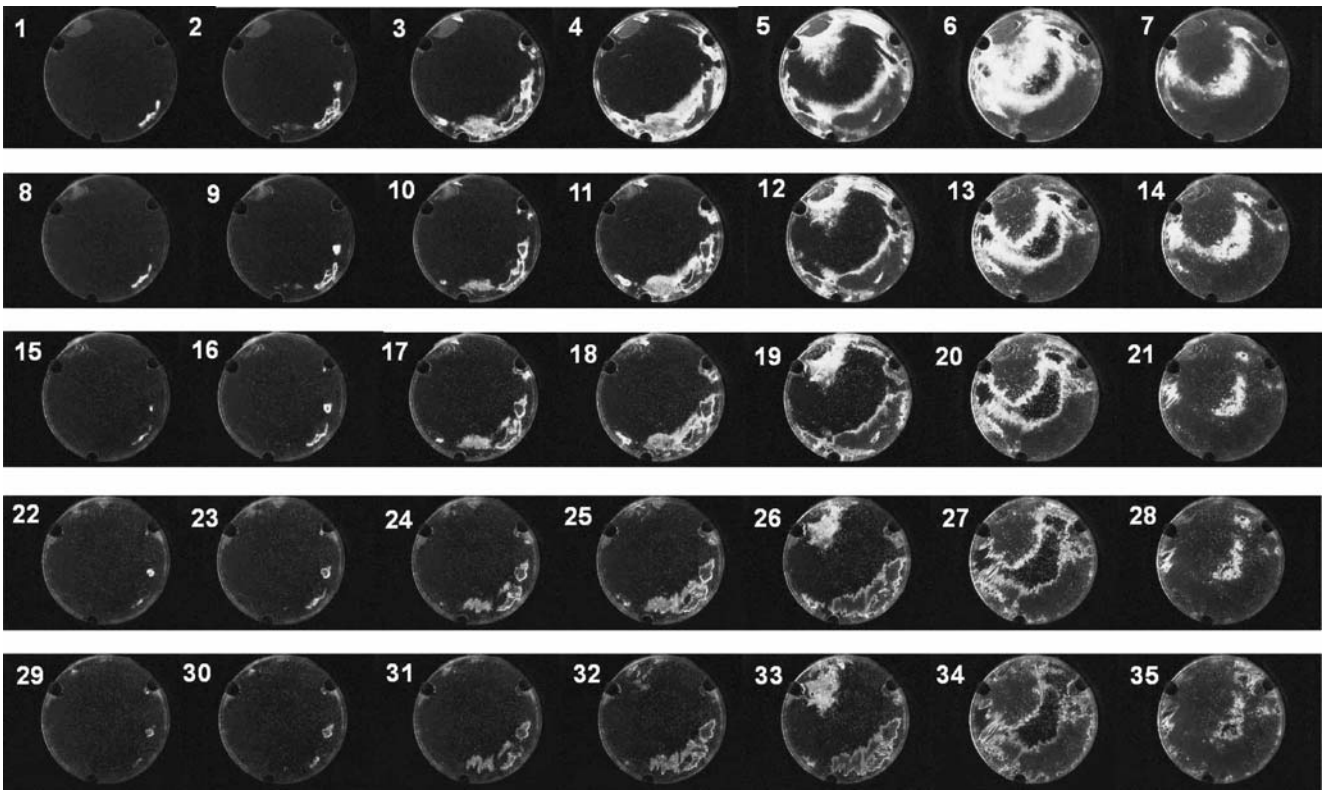

Fig. 15 Periodic development of the luminescent spatiotemporal patterns in the thin layer (d=1.29 mm) of the solution in which thiocyanate anions are oxidized with hydrogen peroxide in an alkaline medium, in the presence of Cu^{2+} ions as a catalyst. *Bright areas* correspond to blue luminescence of luminol, appearing on the *black* (dark solution) background (reprinted with permission from [13], Copyright 2007 American Chemical Society)

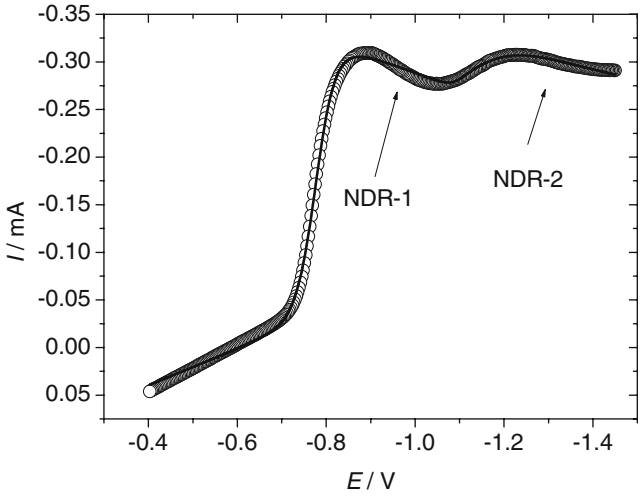

Fig. 16 The steady-state current–potential characteristics of the $Ni(II) - N_3^-$ electroreduction (in a slightly acidified solution) at the streaming mercury electrode, exhibiting two regions of the negative differential resistance (*NDR-1*, *NDR-2*; reprinted in part with permission from [14], Copyright 2003, American Chemical Society)

of control parameters. Similarly, as for bistability, the electric circuit requires then the presence of the appropriate ohmic potential drops and for that it was necessary to insert an external ohmic resistor in series with the working (here: streaming) electrode (Fig. 17).

One should strongly emphasize that although it is easy to define theoretical conditions for tristability, their realization in practice is much more difficult. Therefore, although numerous examples of electrochemical bistable systems can be found in the literature, the reports on tristability are very rare.

To our best knowledge, before our paper [14], there were only a few reports by Schell on the tristable characteristics of anodic oxidation of some alcohols on Pt electrode (cf., [17]). Therefore, it appears that the electroreduction of the azide complexes of nickel(II) is only a second example of tristability in electrochemistry. If we add that in homogeneous oscillators, the tristability was found only for three experimental systems [18–20]; it becomes clear how really rare the experimental manifestations of this complex behavior are. Figure 18 shows the *I–E* characteristics for zero serial resistance R_s and the corresponding bistable and tristable behaviors observed for nonzero resistances, for the electroreduction of azide complexes of nickel(II) at the streaming mercury electrode.

Application of nonlinear dynamics in materials science

During the synthesis of materials of desired properties, all kinds of dynamical instabilities described above can manifest themselves. The fundamental question that can be immediately posed is the following: Are such instabilities only a nuisance, or can they be useful for the synthesis of new materials? The answer is that both cases are possible. If the process in a reactor, particularly in a large industrial scale, spontaneously starts to proceed in an oscillatory manner against our intentions, it means that we lose control over the reaction course; in an extreme case, such situation can even lead to the damage of the reactor. However, if we are familiar with nonlinear dynamics and thus understand the cause for such behavior, we can appropriately optimize the reactor construction or conditions of the reactions, to avoid such undesirable situation.

However, there are also possible evident advantages that we can take from the dynamical instabilities in *designing new materials*. In this review, we mention selected but representative examples of such situations. The examples come from the polymer chemistry [2, 21–23] and from electrochemistry.

Examples of nonlinear dynamics in polymer chemistry

Concerning polymerization reactions, one can distinguish between two essentially different aspects of the role of nonlinear dynamics in such processes [4]:

1. The polymerization process itself may exhibit nonlinear instabilities, due to intrinsic nonlinearities and feedback loops.
2. The polymerization process does not exhibit such instabilities but is *coupled* with the oscillatory chemical system, like the famous BZ process.

These two cases will be now briefly exemplified.

Dynamic instabilities in polymerization reactions

A representative example of the feedback leading to instabilities is the *thermal autocatalysis*, which means that the exothermic process causes the rise of temperature, which accelerates further the exothermic reaction and so on (the situation is quite typical of the free radical polymerization). Such feedback can set in easily in large industrial reactors because of their low surface-to-volume ratio (the heat produced in the bulk of the reactor has little chance to

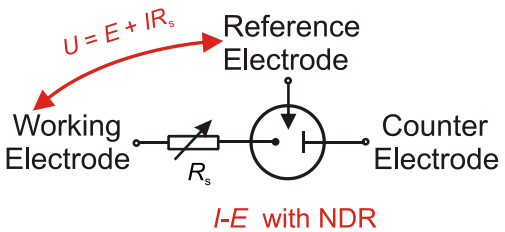

Fig. 17 Typical circuit for the measurements of electrochemical instabilities associated with the negative differential resistance (*NDR*) in the *I–E* characteristics of the process

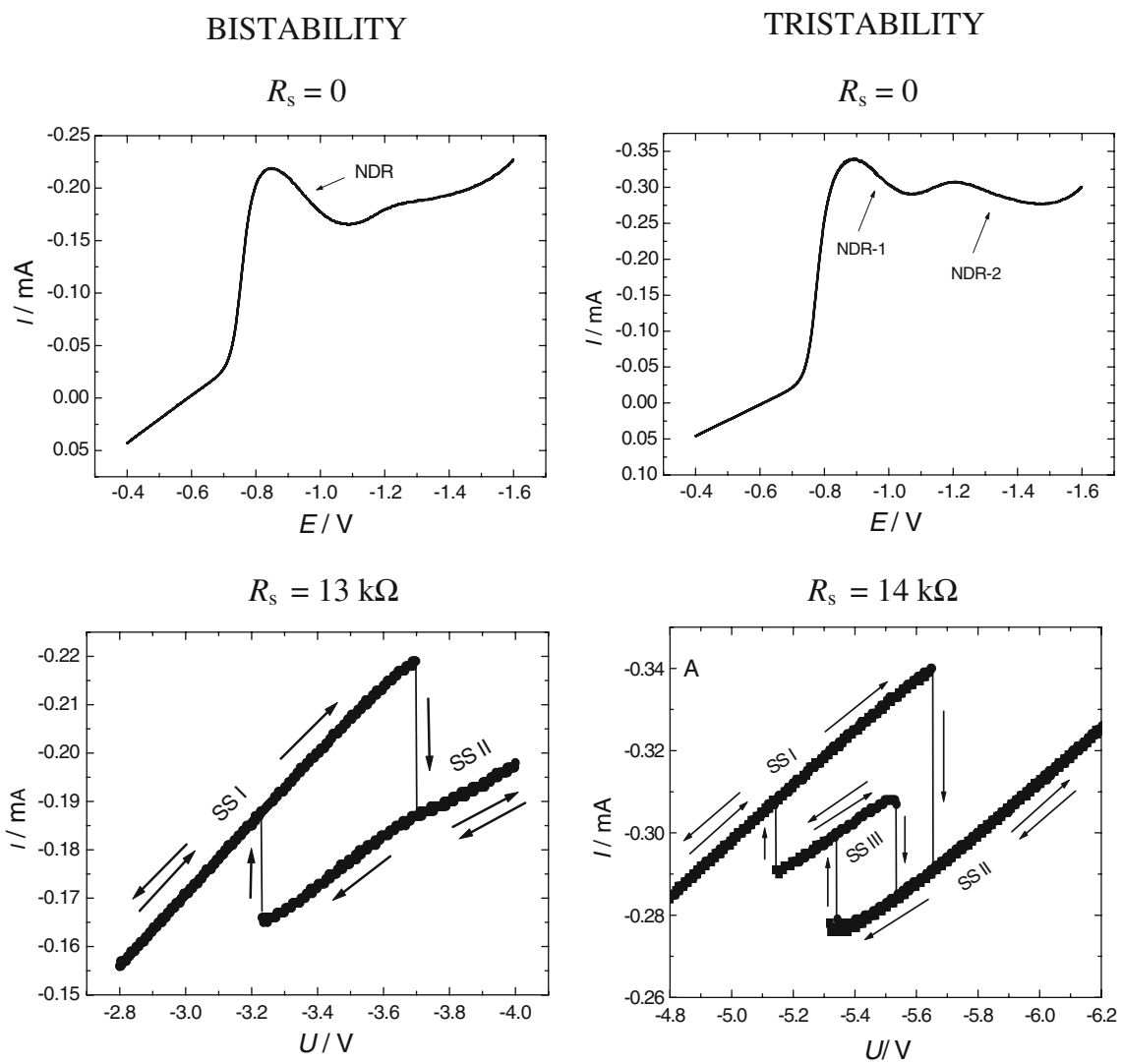

Fig. 18 Bistability and tristability observed for the $Ni(II) - N_3^-$ electroreduction at the streaming Hg electrode, for two compositions of the samples; *left column*: 2.0 mM $Ni(ClO_4)_2$+1 M NaN_3+6 mM $HClO_4$, *right column*: 4.0 mM $Ni(ClO_4)_2$+2 M NaN_3+12 mM $HClO_4$ (reprinted in part with permission from [14], Copyright 2003 American Chemical Society)

leave quickly to the surroundings). Another type of the feedback is possible under isothermal conditions: With the increase of the length of radical polymeric chains, the viscosity of the medium increases; the diffusion-limited transport of such chains toward each other is then slowed down, so the probability of their meeting and thus recombination, terminating further chain propagation, also decreases. As a result of this increasing viscosity, the rate of polymerization increases [2].

In some free radical polymerization processes, the coupling of these two effects may lead to oscillations. As a function of time, the reaction is autocatalytically accelerated due to the temperature rise. This, however, causes the decrease in medium viscosity. The faster diffusion of radical chains increases the probability of their meeting and recombination. This in turn means termination and the decrease in the rate of the polymerization reaction. If the direct acceleration of the polymerization through the temperature rise and its inhibition through the effect of decreasing viscosity occur in different time scales, the kinetics of the whole process attains the oscillatory character, manifesting itself, e.g., by the oscillatory variations of the temperature of the reaction mixture [2]. The oscillatory course of the free radical polymerization of vinyl acetate (with the period of oscillations approximately 100 min and the amplitude of the temperature changes close to 15–20°) can serve as an example [24].

According to recent trends in nonlinear dynamics, which devotes much attention to the spatial and spatiotemporal dissipative structures, also polymerization processes can produce such patterns. The most trivial case occurs upon very fast removal of the solvent, as a result of which the nonequilibrium ("freezed") pattern emerges from the system. However, much more sophisticated and useful is

the phenomenon of the *frontal polymerization* in which the reaction zone propagates in the reactor space through the coupling of thermal diffusion and Arrhenius-type reaction kinetics. By changing the conditions of such experiments, one can modify the progress of the fronts, which allows one to produce polymer materials of unique, desired morphologies [2, 22]. The frontal polymerization can be performed both in radical reactions and epoxy curing. The frontal polymerization of *n*-butyl acrylate with azobisisobutyronitrile can serve as a representative example of such a process [25].

It is noteworthy that in polymerization reactions, similarly as in homogeneous and heterogeneous chemical oscillatory processes, also spiral spatiotemporal patterns were observed.

Polymerization coupled to the oscillatory chemical reactions

For the creation of such coupling, the oscillatory BZ reaction is often used. For example, if acrylonitrile is added to the solution containing BZ reagents, one observes the onset of acrylonitrile polymerization only when the oscillatory regime of the BZ process sets in (Fig. 19). Furthermore, the oscillatory polymerization occurs in phase with the BZ oscillations.

Detailed studies of these phenomenon have revealed that this coupling was caused by periodic termination of polymerization by bromine dioxide, which concentration exhibited oscillatory variations as a function of time.

In another variant of such a coupled (BZ–polymer) system, the solution contains all the BZ reactants, except

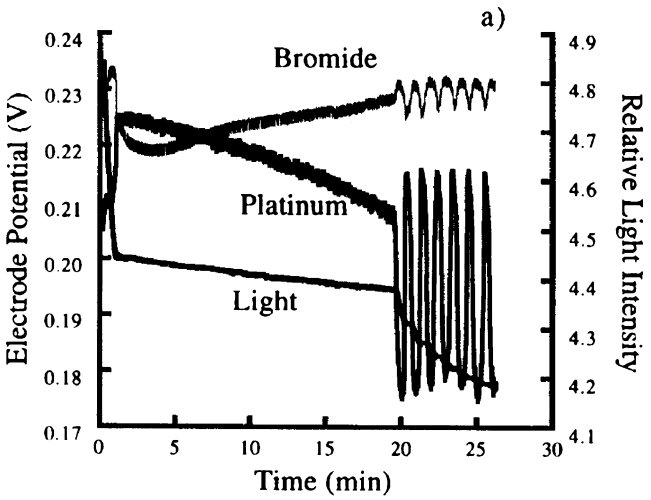

Fig. 19 The coupling between the onset of oscillations in the cerium-catalyzed BZ reaction and the polymerization of acrylonitrile. The BZ reaction is monitored with the Pt and the ion-selective electrode sensitive to bromide concentrations, while the turbidity of the sample shows the progress of polymerization (reprinted in part with permission from [32], Copyright 1992 American Chemical Society)

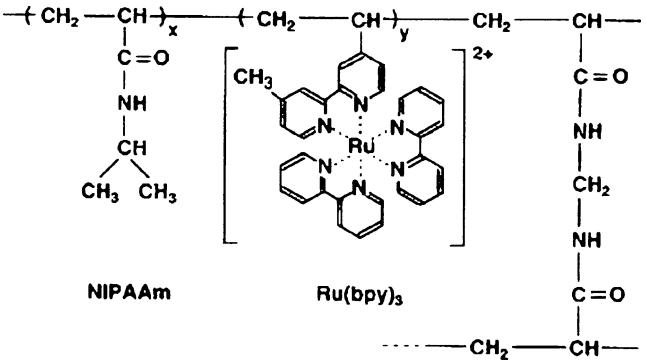

Fig. 20 The chemical structure for the poly[NIPAAm-co-Ru(bpy)$_3$] gel (reused with permission from [26], copyright 1999, American Institute of Physics)

for the ions of the catalyst, which are covalently bound to the polymer chain. If such a polymer, modified e.g. with the appropriate complex of Ru(III) ions (cf. Fig. 20), is brought into contact with the solution containing other BZ reagents, the periodic changes of the oxidation state of ruthenium ions, associated with the change in the hydration shells of these ions, cause the periodic changes of the direction of the transport of water molecules: either inside the gel (when ruthenium attains a +3 oxidation state) or outside the gel (for Ru^{2+} ions) [26]. As a consequence, the gel phase exhibits alternating swelling and deswelling (Fig. 21). In addition, since the color of complex compounds of ruthenium depends on the oxidation state of the central ion, simultaneous periodic changes of the gel color are observed.

The potential application of such phenomena includes the developing of new micromachines, like "peristaltic micropumps." Recently, an analogous approach was applied to the system, in which the gel phase consisted of a

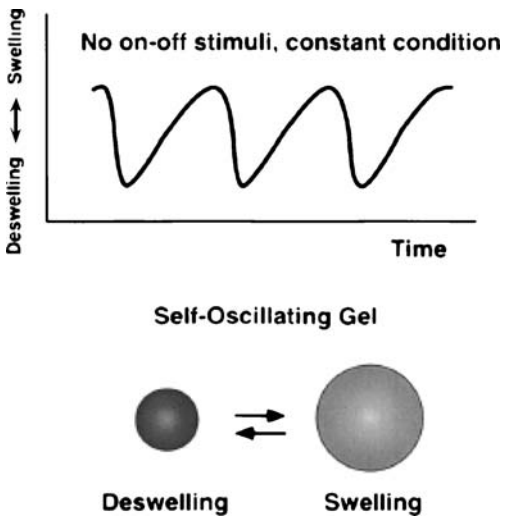

Fig. 21 Self-induced oscillations of the modified gel from Fig. 20, in contact with the solution containing other reagents of the BZ reaction (reused with permission from [26], copyright 1999, American Institute of Physics)

little colloidal particle, called then the "colloidal photonic crystal" [27]. In this way, the idea of coupling of the polymer phase changes with the oscillatory reaction entering the world of nanomaterials.

Other examples of the oscillatory processes in gel media include, among others, bistability and complex oscillations reported for the acid–base–acid transistors [28] and the surface micropatterning using the so-called wet-stamping technique [29, 30], applied, e.g., to the periodic precipitation processes [31], mentioned above as the historical Liesegang phenomena.

Evidently, the coupling of the polymerization and oscillatory phenomena opens new ways of preparations of the nanomaterials. However, to obtain the precisely designed materials, one has not only to elaborate the proper experimental conditions but also to understand the mechanism of these phenomena. Therefore, recently, more and more attention is being devoted to the eventual coupling between the dynamic (nonequilibrium) self-organization described in this presentation and the local self-assembling phenomena ruled by the tendency of the system to reach the minimum of Gibbs energy (equilibrium state) [32].

Examples of nonlinear dynamics in the electrochemical preparation of nanomaterials

Generally, the importance of nanoscale materials is caused by the fact that their optical, electrical, chemical, and mechanical properties may be tuned by changing the size of the materials [33]. Electrochemical methods are one of the most efficient methods of synthesis of nanomaterials. For that purpose, one may use either electrodeposition or electrodissolution (etching) processes, involving both metals and semiconductors.

Switzer et al. [33–35] have described the formation of the nanoscale multilayers of Cu/Cu_2O during their galvanostatic cathodic electrodeposition, associated with the spontaneous oscillations of the electrode potential. Since the thickness of Cu_2O layers appeared to be less than 3 nm, for their analysis, it was difficult to use electron microscopy, but the electrochemical quartz crystal microbalance technique, compared with bulk X-ray diffraction measurements, allowed the authors to study in more detail the phase compositions of the Cu/Cu_2O layers and the effect of various experimental factors on their formation. For example, the phase composition of the electrodeposited Cu/Cu_2O films appeared to be strongly dependent on the applied current density [34]: An increase in the current density could tune the layer composition from practically pure Cu_2O to a predominating content of Cu over Cu_2O. Furthermore, it was suggested that the deposition of only Cu_2O occurs when the oscillating electrode potential attains relatively positive values (in the form of sharp spikes), while the common deposition of the $Cu+Cu_2O$ composite takes place during the longer periods when, between the positive spikes, the electrode potential attains the relatively negative value.

The periodically nanostructured copper filaments self-organized by electrodeposition have been described recently also by Wu et al. [36]. Due to spontaneous oscillations of the concentration field of the Cu^{2+} ions in the front of the growing interface, crystallites of copper and cuprous oxide appeared alternatively on the filaments of the electrodeposits. Using conducting atomic force microscopy and current imaging tunneling spectroscopy, it was found that despite the periodic distribution of Cu_2O crystallites on the deposited filament, there should exist a metallic core of copper crystallites inside the filament. In the authors' opinion, this type of structure of a metal–semiconductor filament might have potential practical applications.

The spontaneous oscillations in the electrochemical deposition of copper, leading to layered nanostructures, were modeled in terms of a new Monte Carlo model [37], with the emphasis on the correspondence between the oscillation of pH and the layered structure.

Concerning further Cu electrodeposition, one should note that Najanishi et al. [38] found the new type of the hidden N-shaped NDR in the layer-by-layer electrodeposition of copper from aqueous acidic Cu^{2+} solutions in the presence of *o*-phenanthroline. The NDR region is caused by the adsorption of the reduced form of the copper(II) complex with *o*-phenanthroline, which suppresses the Cu electrodeposition. Both potential and current oscillations were reported and associated with the layered structure of Cu deposit, with the layer thickness of about 5 μm. The increase in the current is caused by the increase in the effective electrode area by growth of the thin Cu leaflets.

Electrodeposition of zinc is another process studied from the point of view of pattern formation at the electrodes. Wang et al. [39, 40] observed the self-organization of periodically structured single-crystalline zinc branches by its electrodeposition from an ultrathin aqueous layer of the $ZnSO_4$ solution. Each branch of the deposit appeared to be made of periodic bead-like structures, and a layered morphology has been observed on each bead. Under conditions of a constant voltage, there were observed spontaneous current oscillations, associated with the formation of periodic patterns on deposit branches. The interpretation of these phenomena involved the idea of the epitaxial nucleation in the transport-limited growth system.

Concerning further zinc electrodeposition, Fukami et al. [41] have described the self-organized periodic growth of stacked hexagonal wafers. A strongly alkaline Zn(II) solution was used, and the oscillations of the electrode potential were observed in the region of current density exceeding the diffusion-limited value. Furthermore, scan-

ning electron microscopic inspection showed that the dendrites formed changed their shape periodically, in synchronization with the oscillations of the electrode potential—from thick hexagonal wafers at the relatively negative potentials to thin maple-leaf-like hexagonal wafers at relatively positive potentials. Simultaneously, the rate of zinc electrodeposition also oscillated. The mechanism explaining these phenomena assumed coupling of the autocatalytic Zn crystal growth and autocatalytic surface oxidation at the close-packed crystal faces leading to surface passivation.

Following these studies of electrodeposition of single metals, we shall note some papers related to the codeposition of various metals. Sakai et al. [42] have studied the mechanism of oscillations and the formation of nanoscale-layered structures in induced codeposition of some iron-group alloys (Ni–P, Ni–W, Co–W). Such structures have unique properties and are widely used in industries. It is interesting to note that the quartz microbalance studies have revealed that the induced codeposition of the alloys exhibits the NDRs, which are a source of oscillations and structure formation. Furthermore, due to an overlap of the deposition current with the hydrogen evolution current, this negative resistance may remain hidden. These findings led to the development of the general mechanism for the induced codeposition of these industrially important materials.

Furthermore, Nakato et al. [43, 44] have described the formation of the macroscopically uniform nanoperiod alloy multilayers formed by the coupling of electrodeposition with current oscillations, for the acidic solution of Cu^{2+}, Sn^{2+}, and a cationic surfactant. The electrochemical characteristics of such a system exhibited a NDR, coming from the adsorption of a cationic surfactant (acting as an inhibitor for diffusion of metal ions) on the alloy surface. Obviously, the coupling of the NDR with the ohmic drops in the electrolyte was a source of observed dynamical instabilities. Scanning Auger microscopic inspection proved that the alloy films deposited during the oscillations had an alternate multilayer structure composed of two alloy layers of different compositions.

There is also a series of papers devoted to electrodeposition of metal or nonmetals on semiconducting surfaces. Nagai et al. [45] have described apparently the first example of the open-circuit potential oscillations observed on semiconductor electrode (here: *p*-Si) during the electronless Cu deposition from the $HF+CuSO_4$ solution. The oscillations appeared only when the Cu deposit formed a continuous porous film composed of mutually submicrometer-sized particles. In the explanation of these oscillations, the key role was ascribed to the coupling between the autocatalytic shift in the flat-band potential of Si, caused by the change in the coverage of the Si oxide and the connection and disconnection of the Cu film with the Si surface.

In addition, Nakato et al. [46] have described the nanosized structures of the atomically flat semiconductor and metal surfaces, formed by chemical and electrochemical methods. The formation of these nanosized structure was caused by the self-organized organizing abilities of molecular and nanosized systems. One of the examples included the formation of nanoholes at atomically flat, H-terminated *n*-Si(111) surfaces, which occurred during electrochemical deposition of Pt (this means the reductive dissolution of Si surface, catalyzed by Pt in an intermediate monoatomic state). Other examples included the formation of ordered iodine nanorods on the H-terminated *n*-Si(111) surfaces and the formation of ordered arrays of gold nanoparticles in aqueous solutions and on Au(111) surfaces. The latter phenomena occur upon the addition of organic thiols to particle solutions, and the aspect ratio of the ordered arrays depended on the kind of thiols added. In conclusion, chemical and electrochemical methods were suggested as the powerful approaches to the production of ordered nanostructures on solid surfaces.

The abovementioned papers turn further the attention on the electrochemical etching of semiconductors. This is one of the subjects quite intensively studied over the last decades in the area of electrochemical nanostructuring. The semiconductors used include, among others, electrochemically nanostructured GaAs and CdSe, which are important, e.g., for the development of optoelectronic devices. Recently, Tiginyanu et al. [47] have shown that in the electrochemical nanostructuring of GaAs and CdSe, their porosification can be controlled by the conditions of anodic etching in the aqueous solution of NaCl, the medium that is relatively nonaggressive, compared to commonly used strong acids or alkaline electrolytes. Obviously, silicon is another important semiconductor, the microstructuring of which is intensively studied. Tiginyanu et al. described the electrochemical etching of silicon, which process, apart from important technical applications, is an interesting experimental setup for self-organized structure formation capable, e.g., of regular, diameter-modulated, and branching pores. The anodic polarization of Si in a diluted HF solution causes the generation of a porous silicon layer, followed by its oxidation and electropolishing, and, at more anodic potentials, by the oscillatory regime [48–50]. Depending on the experimental electrochemical conditions, reflected also in the model, completely different surface morphologies can be produced. For example, by increasing the HF concentration (which means faster Si oxide dissolution and thus its diminished effect), the electropolishing turns first into macropore (several micrometers) formation and then into mesopore formation (strongly anisotropic, narrow pores with diameters less than 400 nm). The important role of passivation and different aging of surfaces in different crystallographic orientations

in the pore morphologies was indicated. In addition, the lateral pore interaction appeared to induce further modification of different morphologies obtained. From the theoretical point of view, invoking the concepts of nonlinear dynamics, the pore formation during the silicon etching was explained in terms of the current-burst model [51–53]. In the opinion of the authors [48], the model of this type seems to reflect a number of quite general properties of semiconductor electrochemistry.

Another interesting aspect of this approach is the possibility of the control of the dynamics of the pore formation, which does not involve the feedback, contrary to the well-known approaches of Ott et al. [54], as well as of Pyragas [55]. The goal of such control is technically important, as the pore diameter should not exceed 500 nm. The idea of the appropriate open-loop stabilization involves the modulation of the experimental parameters, e.g., of the etching current.

Concerning the InP semiconductor, one should mention the work by Langa et al. [56] in which the self-organized single-crystalline two-dimensional hexagonal arrays of pores were reported. More precisely, such self-arrangement of pores was observed for *n*-type substrates with (100) and (111) orientations. Both randomly distributed nanopores (belonging to the nucleation layer of the crysto-pores, forming first) and curro-pores, either with short-range or long-range ordering, were observed. Both crysto- and curro-pores showed manifestations of pattern formation. Furthermore, under galvanostatic conditions, spontaneous voltage oscillations were observed, which correlate with the self-induced synchronized diameter oscillations of curro-pores in a (111)-oriented sample.

Furthermore, Föll et al. [57, 58], using the electrochemical pore-etching technique, succeeded in producing deep pores in both *p*-type and *n*-type Ge semiconductors of various doping levels and crystal orientations. The role of various experimental factors, like the electrolyte type, illumination conditions, and pretreatments, was studied. In view of earlier difficulties in obtaining such pores for Ge, these works can be considered the pioneer achievements.

Electrochemical micromachining and dissipative spatiotemporal patterns

Generally, electrochemical micromachining can be achieved by the electrode processes (electrodissolution or electrodeposition) induced locally by using the STM tip polarized with very short potential pulses. In this context, one should invoke remarkable approach, elaborated in the group of Ertl, the Nobel Prize laureate in 2007. The principle of the method suitable for three-dimensional machining of conducting material with submicrometer precision is described, e.g., in [59, 60]. The method is based on the finite time constant for double-layer charging, which is linearly dependent on the local separation of the electrodes: one being a tool for micromachining and the other one being the work piece that is to be microstructured. As the tool electrode approaches closely (≤1 μm) the work piece electrode, the local time constant for the double-layer charging is appropriately small, compared to regions when the interelectrode distance is much higher, and so the local ohmic resistance. Upon application of the short-voltage pulse, the electrodes will only be significantly charged where the local time constant does not substantially exceed the pulse duration, which should happen only near the very tip of the tool electrode. Since the rate of the faradaic processes is nonlinearly, i.e., exponentially dependent on the potential drop in the double layer, the electrodissolution or electrodeposition processes (depending on the system chosen and the voltage applied vs. the equilibrium potential of a given redox couple) are confined practically to the electrode regions in close proximity to the tool. In this way, it was possible to cause etching of the Cu substrate with the formation of, e.g., the Cu prism 5×10×12 μm. In turn, on the Au substrate and using an elliptical Pt tool 50 μm in diameter, it was possible to deposit Cu dots from the acidified solution of $CuSO_4$. This method of electrochemical micromachining can be applied to all electrochemically active materials, including semiconductors. A hole etched in *p*-Si with a cylindrical 50-μm tool in 1% HF can serve as an example [59].

As this review is essentially devoted to nonlinear dynamics, one should indicate its specific significance of this kind of dynamics in the pattern formation in heterogeneous systems. One of the most intensively studied processes that exhibits wealth of various instabilities is the catalytic oxidation of CO on various platinum surfaces (cf. [61–63]). From the most recent studies, one may invoke, for example, the paper by Bertram et al. [64] who have described the formation of complex patterns on the Pt(110) single-crystal surface upon variation of the forcing amplitude and frequency. Applying the global delayed feedback to this system resulted in the suppression of chemical turbulence and the formation of different patterns, including intermittent turbulence, oscillatory standing waves, cellular structures, and phase clusters [65, 66].

In the electrochemical systems, the spatiotemporal evolution of the double-layer potential is the key phenomenon underlying any structure formation. Another key idea is the nonlocal and practically instantaneous coupling of the different parts of the electrode, since the local variation of the double-layer potential will affect the potential distribution, as well as the electric field across the whole electrolyte. This in turn affects local migration currents at any point of the electrode surface. A general model for the spatial pattern formation according to this mechanism was

developed by Flätgen and Krischer [67], and its experimental verification involved, among others, studies of the potentiostatic reduction of $S_2O_8^{2-}$ at an Ag ring electrode [68].

Finally, one should emphasize the recent success in obtaining the stationary, i.e., the abovementioned Turing patterns on the electrode surfaces, which may open further ways toward fabrication of structured electrodes. The idea is that one of the conditions for the formation of such structures, the difference in transport properties of the activator and the inhibitor engaged in the oscillatory process, can be realized in this way that the electrode potential acts as an inhibitor, while the rate of migration transport can be varied by the electrode potential, easily exceeding the rate of diffusion transport for even orders of magnitude [60, 69–71].

To conclude, as stated above, this paper summarizes only basic concepts of nonlinear dynamics and collects selected examples of its manifestation in the processes that are important from the point of the materials science. However, even from this concise presentation, one can easily conclude that the connection between the nonlinear dynamics and materials science is a modern, promising, and challenging discipline.

References

1. Scott SK (1994) Oscillations, waves and chaos in chemical kinetics. Oxford University Press, London
2. Epstein IR, Pojman JA (1998) An introduction to nonlinear chemical dynamics. Oxford University Press, Oxford, NY
3. Orlik M (1996) Oscillating reactions—order and chaos. WNT, Warsaw (in Polish)
4. Kawczyński AL (1990) Chemical reactions—from equilibrium, through dissipative structures to chaos. WNT, Warsaw (in Polish)
5. Williams R (1963) J Chem Phys 39:384
6. Schaper H, Köstlin H, Schnedler E (1982) J Electrochem Soc 129:1289
7. Orlik M, Rosenmund J, Doblhofer K, Ertl G (1998) J Phys Chem B 102:1397
8. Orlik M, Doblhofer K, Ertl G (1998) J Phys Chem B 102:6367
9. Orlik M (1999) J Phys Chem B 105:6629
10. Orlik M (1999) PCCP 1:5359
11. Orlik M (2000) Electrochem Commun 2:522
12. Orbán M (1986) J Am Chem Soc 108:6893
13. Pękala K, Jurczakowski R, Lewera A, Orlik M (2007) J Phys Chem A 111:3439
14. Jurczakowski R, Orlik M (2003) J Phys Chem B 107:10148
15. Jurczakowski R, Orlik M (2002) J Phys Chem B 106:1058
16. Jurczakowski R, Orlik M (2005) J Electroanal Chem 574:311
17. Schell M (1998) J Electroanal Chem 457:221
18. Orbán M, Dateo C, De Kepper P, Epstein IR (1982) J Am Chem Soc 104:5911
19. Nagy A, Treindl L (1989) J Phys Chem 93:2807
20. Chie K, Okazaki N, Tanimoto Y, Hanazaki I (2001) Chem Phys Lett 334:55
21. Ray WH, Villa CM (2000) Chem Eng Sci 55:275
22. Epstein IR, Pojman JA (1999) Chaos 9:255
23. Pojman JA, Trang-Cong-Miyata Q (eds) (2002) Nonlinear dynamics in polymeric systems. ACS Symposium Series no. 869. Oxford University Press, New York
24. Teymour F, Ray WH (1992) Chem Eng Sci 47:4121
25. Khan AM, Pojman JA (1996) Trends Polym Sci 4:253
26. Yoshida R, Kokufuta E, Yamaguchi T (1999) Chaos 9:260
27. Takeoka Y, Watanabe M, Yoshida R (2003) J Am Chem Soc 125:13320
28. Hegedüs L, Kirschner N, Wittmann M, Simon P, Noszticzius Z, Amemiya T, Ohmori T, Yamaguchi T (1999) Chaos 9:283
29. Campbell CJ, Smoukov SK, Bishop KJM, Grzybowski BA (2005) Langmuir 21:2637
30. Bishop KJM, Fiałkowski M, Grzybowski BA (2005) J Am Chem Soc 127:15943
31. Bensemann IT, Fiałkowski M, Grzybowski BA (2005) J Phys Chem B 109:2774
32. Ishikawa M (2005) Chaos 15:047503
33. Bohannan EW, Huang LY, Scott Miller F, Shumsky MG, Switzer JA (1999) Langmuir 15:813
34. Switzer JA, Hung CJ, Huang LY, Miller FS, Zhou Y, Raub ER, Shumsky MG, Bohannan EW (1998) J Mater Res 13:909
35. Huang LY, Bohannan EW, Hung CJ, Switzer JA (1997) Isr J Chem 37:297
36. Wu Z, Bao YJ, Yu GW, Wang M, Peng RW, Fleury V, Hao XP, Ming NB (2006) J Phys Condens Matter 18:5425
37. Ha MJ, Fang F, Liu JM, Wang M (2005) Eur Phys J D 34:195
38. Najanishi S, Sakai S, Nishimura K, Nakato Y (2005) J Phys Chem B 109:18846
39. Liu T, Wang S, Wang M, Peng RW, Ma GB, Hao XP, Ming NB (2006) Surf Interface Anal 38:1019
40. Wang S, Zhang KQ, Xu QY, Wang M, Peng RW, Zhang Z, Ming NB (2003) J Phys Soc Jpn 72:1574
41. Fukami K, Nakanishi S, Tada T, Yamasaki H, Sakai S, Fukushima S, Nakato Y (2005) J Electrochem Soc 152:C493
42. Sakai S, Nakanishi S, Nakato Y (2006) J Phys Chem B 110:11944
43. Sakai S, Nakanishi S, Fukami K, Nakato Y (2002) Chem Lett 6:640
44. Nakanishi S, Sakai S, Nagai T, Nakato Y (2005) J Phys Chem B 100:1750
45. Nagai T, Nakanishi S, Mukouyama Y, Ogata YH, Nakato Y (2006) Chaos 16:037106
46. Nakato Y, Murakoshi K, Imanishi A, Morisawa K (2000) Electrochemistry 68:556
47. Tiginyanu IM, Ursaki VV, Monaico E, Foca E, Föll H (2007) Electrochem Solid State Lett 10:D127
48. Claussen JC, Carstensen J, Christophersen M, Langa S, Föll H (2003) Chaos 13:217
49. Föll H (1991) Appl Phys A Solids Surf 53:8
50. Smith RL, Collins SD (1992) J Appl Phys 71:R1
51. Carstensen J, Christophersen M, Föll H (2000) Mater Sci Eng B 69–70:23
52. Carstensen J, Prange R, Popkirov GS, Föll H (1998) Appl Phys A Mater Sci Process 67:459
53. Carstensen J, Prange R, Föll H (1999) J Electrochem Soc 146:1134
54. Ott E, Grebogi C, Yorke JA (1990) Phys Rev Lett 64:1196
55. Pyragas K (1992) Phys Rev Lett A 170:421
56. Langa S, Tiginyanu IM, Carstensen J, Christophersen M, Föll H (2003) Appl Phys Lett 82:278
57. Cheng F, Carstensen J, Föll H (2006) Mater Sci Semicond Process 9:694
58. Fang C, Föll H, Carstensen J (2006) J Electroanal Chem 589:259
59. Schuster R, Kirchner V, Allongue P, Ertl G (2000) Science 289:98
60. Ertl G (2002) Faraday Discuss 121:1

61. Imbihl R (1993) Prog Surf Sci 44:185
62. Strasser P, Lübke M, Raspel F, Eiswirth M, Ertl G (1997) J Chem Phys 107:979
63. Ertl G (1997) Appl Surf Sci 121:20
64. Bertram M, Beta C, Rotermund HH, Ertl G (2003) J Phys Chem B 107:9610
65. Bertram M, Beta C, Pollmann M, Mikhailov AS, Rotermund HH, Ertl G (2003) Phys Rev E 67:036208
66. Kim M, Bertram M, Pollmann M, von Oertzen A, Mikhailov AS, Rotermund HH, Ertl G (2001) Science 292:1357
67. Flätgen G, Krischer K (1995) J Chem Phys 103:5428
68. Flätgen G, Krischer K (1995) Phys Rev 51:3997
69. Mazouz N, Krischer K (2000) J Phys Chem B 104:6081
70. Krischer K (2001) J Electroanal Chem 501:1
71. Krischer K, Mazouz N, Flätgen G (2000) J Phys Chem B 104:7545